# Characterization of Near- and Far-Field Radiation from Ultrafast Electronic Systems

Kate A. Remley, *Student Member, IEEE,* Andreas Weisshaar, *Senior Member, IEEE,* Stephen M. Goodnick, *Senior Member, IEEE,* and Vijai K. Tripathi, *Fellow, IEEE*

***Abstract*—Accurate and computationally efficient characterization of near- and far-field radiation from a class of microwave, millimeter wave, and ultrafast systems is presented. A numerical technique is utilized which combines the finite-difference time-domain method with a spatial transformation, the Kirchhoff surface integral. Included in the analysis are inhomogeneous material parameters, small feature size relative to wavelengths of interest, and the wide-band nature of the radiation. Based on simulation results, a simple model of the radiation from an inhomogeneous structure is developed. Finally, the technique is applied to accurately characterize the radiation from a photoconducting structure.**

***Index Terms*— Electromagnetic radiation modeling, FDTD methods, photoconducting devices, ultrafast electronics.**

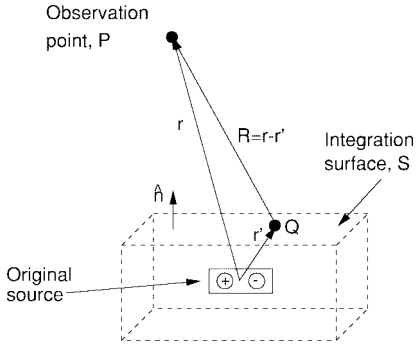


Fig. 1. Equivalent source surface used in the Kirchhoff surface integral.

## I. Introduction

RADIATION from microwave, millimeter wave, and ultrafast electronic systems can be difficult to characterize for a variety of reasons. In general, the radiative source is distributed in nature relative to the wavelength of excitation and may originate from an entire component or region of a component. A variety of material parameters may be involved as well, which can significantly increase the complexity of the characterization. In pulsed millimeter wave and ultrafast electronic systems, the radiation is often wide-band, generally precluding the use of frequency domain techniques. Many of these difficulties can be alleviated through the use of a time domain method such as the finite-difference time-domain (FDTD) technique [1], [2]. However, at very high frequencies, the computational domain becomes excessively large for determination of radiation at distances even relatively near to the source. We apply a technique combining FDTD with a spatial transformation technique, the Kirchhoff surface integral, for determination of near- and far-field radiation from microwave or ultrafast electronic systems. This technique is shown to be very accurate and is often computationally more expedient than use of FDTD alone.

The present work begins with a description of the Kirchhoff surface integral formulation. The method is validated by simulation of simple radiating systems in a homogeneous space for which exact solutions are available. The temporal and spatial characteristics of the Kirchhoff surface integral are discussed in detail. Next, inhomogeneous material parameters are introduced, and their effects on the radiative fields are demonstrated. Finally, results are presented utilizing this technique in the characterization of radiation from a wide-band subpicosecond system. Simulation results show a significantly more accurate portrait of the far-field radiation compared to the standard model for the far field based on the derivative of the source current in which material parameters are not included.

Manuscript received March 27, 1998; revised September 3, 1998. This work was supported by National Science Foundation under Grant ECS-9312240. The work of K. A. Remley was supported in part by a National Science Foundation Graduate Research Fellowship.

K. A. Remley, A. Weisshaar, and V. K. Tripathi are with the Department of Electrical and Computer Engineering, Oregon State University, Corvallis, OR 97331 USA.

S. M. Goodnick is with the Department of Electrical Engineering, Arizona State University, Tempe, AZ 85287 USA.

Publisher Item Identifier S 0018-9480(98)09185-6.

## II. Theory

### A. The Kirchhoff Surface Integral

The Kirchhoff surface integral [3], [4] is one of several near-to-near and near-to-far field transformation techniques [5], [6]. These spatial transformation techniques are based on Huygens' principle, which states that each point on an expanding wavefront may act as a new source of radiation. These techniques allow determination of the electromagnetic fields anywhere in a source-free problem space in terms of known field values on a surface surrounding a calculation volume (see Fig. 1). The Kirchhoff formulation differs from that of other transformation techniques because it is a *scalar* technique, that is, one scalar field quantity is utilized and determined separately in each calculation. For example, $E_z$ at a far-field point is determined only in terms of $E_z$ on the calculation surface.

The Kirchhoff surface integral may be stated as follows: given a homogeneous problem space outside a closed surface $S$, let $\phi(x, y, z, t)$ be a solution of the wave equation whose

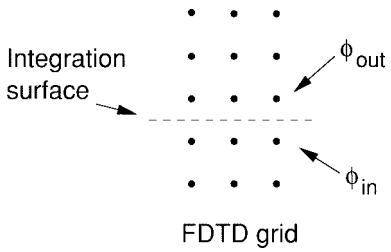


Fig. 2. Implementation of the integration surface in the FDTD code. $\phi$ may refer to any of the six field components in Cartesian coordinates.

first- and second-order partial derivatives are continuous on $S$, and let $P$ be a point outside $S$. Then

$$\phi(P,t) = \frac{1}{4\pi}\int\int_{S'} \times \left\{ [\phi] \frac{\partial}{\partial n'}\left(\frac{1}{R}\right) - \frac{1}{cR}\frac{\partial R}{\partial n'}\left[\frac{\partial \phi}{\partial t}\right] - \frac{1}{R}\left[\frac{\partial \phi}{\partial n'}\right] \right\} dS \tag{1}$$

where the prime refers to points on the integration surface (refer to Fig. 1 for definition of the remaining terms). The square brackets indicate retarded time corresponding to the time required for a signal to travel from a point $Q$ on the surface to $P$ with speed $c = 1/\sqrt{\mu_0 \epsilon_0}$, that is,

$$[\phi] = \phi\left(x', y', z', t - \frac{R_i}{c}\right). \tag{2}$$

As discussed in [7], the Kirchhoff surface integral is easily implemented using the geometry and discretization of a Yee cell-based [1] FDTD code. Using difference equations in time and space, the fields at the integration surface may be calculated from quantities already computed in the FDTD code. The integration surface for a given field component is considered to lie midway between two FDTD gridpoints of the same field component, designated $\phi_{\text{in}}$ and $\phi_{\text{out}}$ in Fig. 2, where $\phi$ may refer to any of the six field components in Cartesian coordinates. The surface field may be calculated efficiently as the mean of values at the two gridpoints, and the normal derivative term in (1) may be found from the difference of these values divided by the distance between them.

The surface integration is implemented as a "time weighted" summation. Time is discretized as $n\Delta t$, with $n$ corresponding to the time step and $\Delta t$ to the time increment. The delay time between each surface element and the observation point, given by $R_i/c$, is precalculated, where the velocity of propagation is taken as the speed of light, $c$. This delay time is used to assign the evolving surface field terms for each surface element to the proper elements of the delayed field vector at each time step [see Fig. 3(a)]. Because the delay time from each surface point to the observation point rarely falls as an integer multiple of $\Delta t$, time interpolation is used. A simple linear interpolation scheme is used for the direct and normal derivative terms, and second-order Lagrangian interpolation is used to maintain second-order accuracy of the time derivative [7].

### *B. Validation of the Technique and Evolution of the Delayed Field Vector*

To illustrate the evolution of the delayed field vector using the FDTD/Kirchhoff integral formulation and to validate the accuracy of the technique, an example is presented comparing the numerical results to the exact solution. The source is a Hertzian dipole excited by a Gaussian current pulse

$$p(n\Delta t) = e^{((n\Delta t - t_0)/\tau)^2} \tag{3}$$

with pulsewidth $\tau = \beta \Delta t$ and delay time $t_0 = 4\tau$. This choice of $t_0$ sets the starting value of the pulse at $\exp(-16) = -140$ dB to minimize noise in the FDTD caused by the turn-on characteristics of the source [8]. With $\beta = 32$ and $\Delta x = \Delta y = \Delta z = 2$ $\mu$m, the time step $\Delta t$ is taken as $\Delta t = 3.47$ fs, which is 0.9 times the Courant stability condition for the FDTD technique. The $E_z$ field component is calculated at observation point $P$, located 60 $\mu$m and 45° off the axis of a $z$-oriented dipole.

The exact solution for the electric field from a Hertzian dipole source is given in many references, for example [9], and will not be repeated here. For the FDTD method, the Hertzian dipole is approximated using the technique described in [10], i.e., the current density is assumed constant over the volume of one grid cell. The field at the integration surface is found using the FDTD technique. To implement the Kirchhoff transformation, at time step $n$ the elements of the delayed field vector [found using (1)] accumulate according to $n\Delta t + R_i/c$. In the time evolution of the delayed field vector, each surface element acts as a secondary elementary source.[1] This is referred to as a time-weighted summation.

As can be seen in Fig. 3(b), agreement between the exact solution and the FDTD/Kirchhoff technique is excellent. Even for simulations in the near-field, such as the present example, the additional calculation time required by the Kirchhoff technique is often offset by the propagation time through the FDTD grid if FDTD was used alone. Additionally, use of the FDTD/Kirchhoff technique reduces the time dispersion associated with the FDTD [11] since the FDTD calculation only extends spatially from the original dipole source to the surface of integration.

### *C. The Components of the Kirchhoff Surface Integral*

In the present work, the combined FDTD/Kirchhoff technique is used to simulate the fields due to nontime-harmonic sources of radiation. It may not be readily apparent how the correct solution is obtained when contributions from the surface integral may arrive at the observation point at times *later* than the duration of the pulse. The way in which the various components of the integral interact can shed light on its apparent nonphysicality. Therefore, in this section two aspects of the evolution of the integral are described—how contributions from the various regions of the integration surface combine, and how contributions from the three terms of the

[1] Because the Kirchhoff surface integral is a scalar technique, each surface element may not be considered as a true "source" of electromagnetic radiation since that would imply a vector quantity. However, the concept of a secondary source describes the time delay accurately.

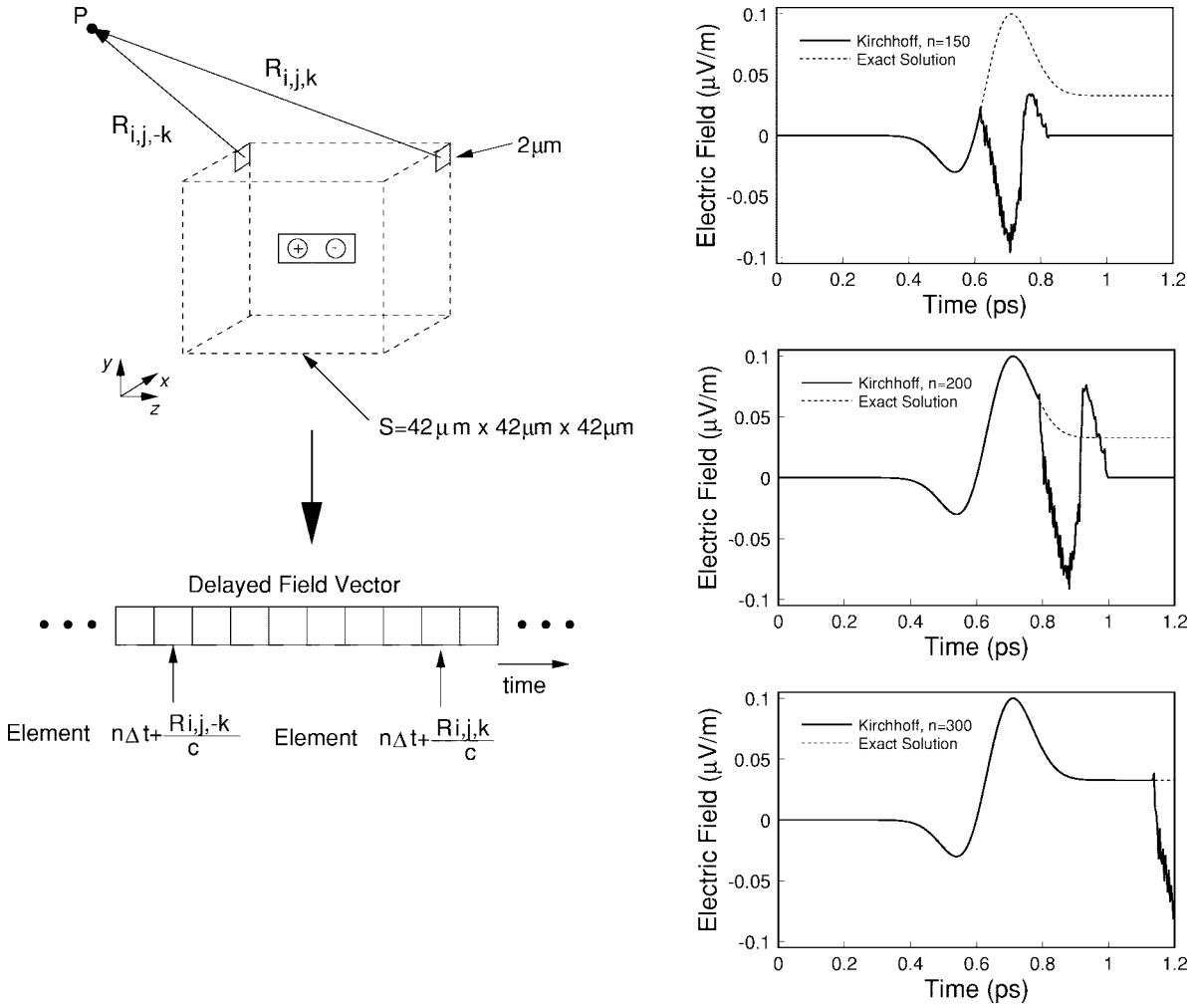


Fig. 3. The delayed field vector. (a) Schematic showing the delay time from each surface element to the observation point. (b) The evolution of the delayed field vector at various time steps $n$ using the Kirchhoff surface integral formulation.

integral combine. Other researchers have utilized the Kirchhoff surface integral formulation in the time and frequency domains [7], [12]–[16]. However, a discussion of the relationships among the various components of the integral has not, to the authors' knowledge, been presented.

In the first case, the contribution from each side of a closed rectangular integration surface similar to that shown in Fig. 3(a) is considered. A scalar (nonelectromagnetic) source is used to present clearly the interrelationships between components of the integral. Excitation is a Gaussian pulse (3) with $\beta = 18$, $\tau = 154$ ps, and $t_0 = 616$ ps. The exact equations for fields at the integration surface from the scalar source were implemented in Matlab [17] with $\Delta x = \Delta y = \Delta z = 0.75$ $\mu$m and $\Delta t = 86.7$ fs. The surface of integration is a cube with 30.75 $\mu$m side dimensions, and the observation point is located 50 $\mu$m directly above the source at the point (0, 50 $\mu$m, 0). Fig. 4 shows that the contribution from the top surface is exact until the time the evolving surface field reaches the edge of the top surface (at approximately 0.23 ps). From this time on, contributions from the top and four sides must be considered collectively. Because the excitation is scalar and centered in the box, the contribution from each of the four sides is equal.

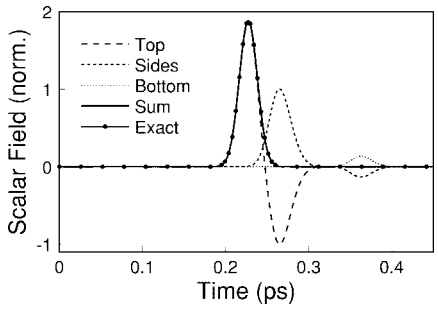


Fig. 4. The time evolution of the contribution from each region of the integration surface. The contributions are summed to yield the complete result of the Kirchhoff surface integral calculation.

Similarly, at around 0.33 ps the contribution from the bottom surface must also be included. Note that components of the received signal have significant value long after the duration of the original pulse.

The contribution from each term of the Kirchhoff surface integral given in (1) is next considered. There are three terms, one of which is directly proportional to the surface field $\phi$, one is proportional to the time derivative of $\phi$, and one is

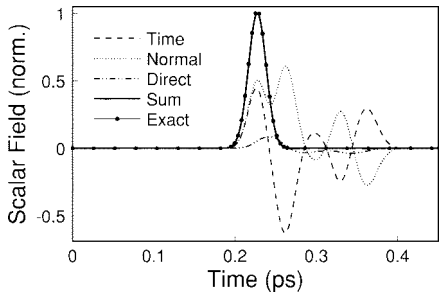


Fig. 5. The time evolution of the $direct$, $time$, and $normal$ terms of the Kirchhoff surface integral.

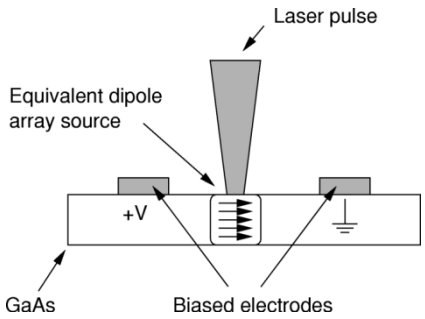


Fig. 6. Typical structure for an electro-optic sampling experiment.

proportional to the normal derivative of $\phi$. These terms will be denoted the $direct$, $time$, and $normal$ terms, respectively. Using the same structure and excitation as in the previous example, the time evolution of each of the three components is displayed in Fig. 5. Because the $direct$ term decreases as $1/R^2$, its contribution to the integral is minimal except in the very near-field. The $time$ and $normal$ terms combine to form the received pulse and cancel at times greater than the received pulse duration. Again, it may be seen that the fields generated at times greater than the pulse effectively cancel to provide the correct solution.

## III. Application of the Method to a Photoconducting Structure

The combined FDTD/Kirchhoff surface integral technique is well suited to the analysis of radiation from a photoconducting structure such as the one shown in Fig. 6. Here, a GaAs substrate is viewed from the side, and two metal electrodes run perpendicular to the plane of the page. A subpicosecond laser pulse is incident on the substrate, creating electron-hole pairs. Application of a bias voltage to the electrodes accelerates the electrons and holes in opposite directions. This produces a time-varying dipole source of radiation oriented parallel to the substrate surface and transverse to the biased electrodes. Such structures may be used in electro-optic sampling applications and in photoconducting switches.

A typical photoconducting structure consists of a GaAs substrate and metal electrodes, as illustrated in Fig. 6. In the following section, the effects of the inhomogeneous material parameters on the radiation characteristics are addressed. The FDTD/Kirchhoff method is first applied to radiation from a GaAs substrate only. Then, analysis of the full photoconducting system is considered.

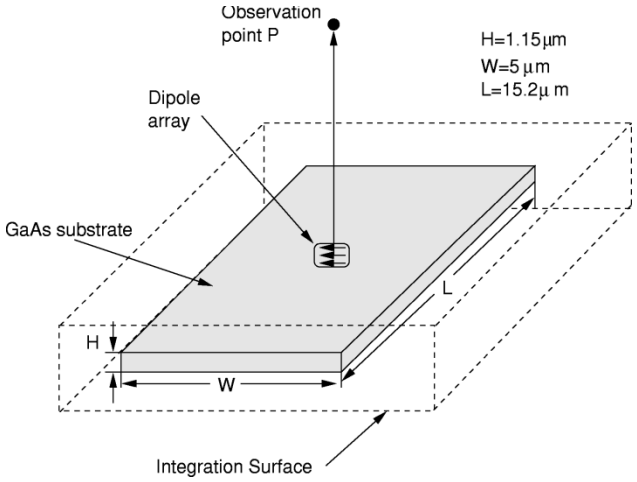


Fig. 7. Structure used to determine the effects of including inhomogeneous material parameters in the simulation. The integration surface is located external to the inhomogeneous problem space.

### A. Inclusion of Inhomogeneous Material Parameters

The extent to which inhomogeneous material parameters significantly alter results depends on several factors, including the temporal characteristics of the excitation relative to the dimensions of the structure and the excitation model used. The effects of these parameters on the radiation are illustrated with a representative structure, again with a Gaussian current pulse excitation. The structure consists of a GaAs substrate with relative permittivity of approximately 12 at the highest frequency involved in the experiment. A worst-case scenario is presented, with absorption equal to zero. The integration surface is placed external to the inhomogeneous material, as discussed in Section II. The dimensions of the structure are shown in Fig. 7. For some applications, such as the photoconducting system, a vertically uniformly distributed current density is assumed in the GaAs substrate. Therefore, the excitation model for this experiment consists of a vertical array of dipoles embedded uniformly in the GaAs substrate, as shown in Figs. 6 and 7. The observation point is 100 $\mu$m above the center of the GaAs substrate, where the received pulse is approaching the far-field response, i.e., the derivative of the current excitation in free space.

Distortion of the received signal occurs when the pulsewidth $\tau$ is narrow enough for reradiation from the air/GaAs interfaces to become resolvable. Results are presented in Fig. 8 for two cases with pulsewidths corresponding to approximately 2/3 ($\tau = 56$ fs) and 1/3 ($\tau = 30$ fs) of the transit time to the far edge of the GaAs substrate, which is 87.8 fs. Also shown are the cases for an ideal Hertzian dipole in free space. For both pulsewidths, diffraction from the edges of the GaAs/air interfaces alters the received electric field. For the narrower pulsewidth, the diffraction additionally causes distortion of the received waveform. These effects would be neglected in a simple current derivative model for far-field radiation.

The edges and corners of the GaAs substrate shown in Fig. 7 effectively act as new sources of radiation. A simple model

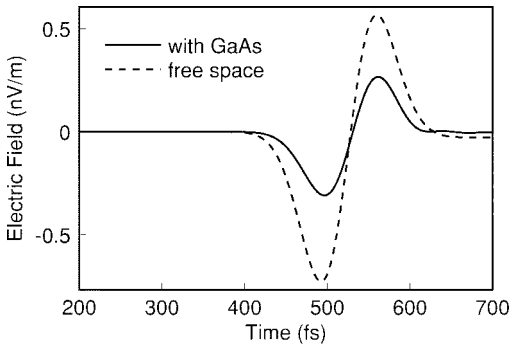


(a)

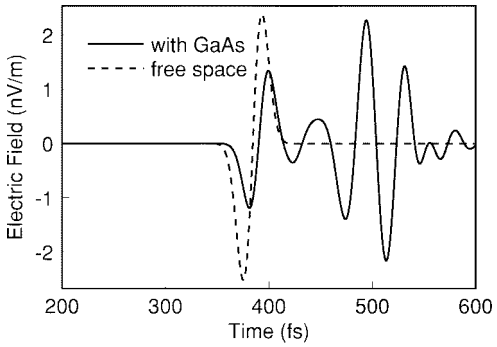


(b)

Fig. 8. Electric field 100 $\mu$m from the source for two different pulsewidths: (a) $\tau = 56$ fs and (b) $\tau = 30$ fs. Transit time to the far edge of the GaAs substrate is 87.8 fs. Dashed lines represent the calculation for an ideal dipole in free space, with an appropriate time delay to account for the presence of the GaAs.

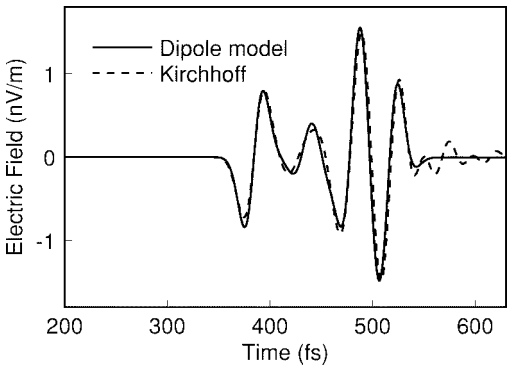


(a)

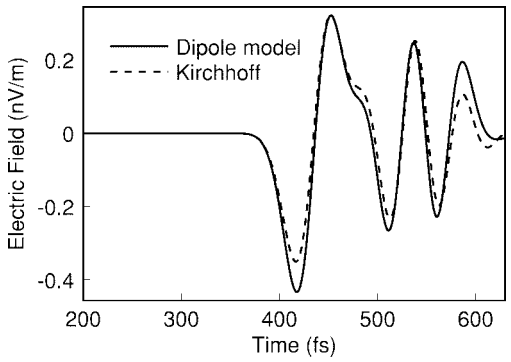


(b)

Fig. 9. Model based on ideal Hertzian dipoles used to represent the reradiation from the corners of the GaAs/air interfaces of the structure shown in Fig. 7. In (a) $\beta = 32$ and (b) $\beta = 64$.

using ideal Hertzian dipoles to represent the diffracting sources has been developed for this structure, based on the simulations using the FDTD/Kirchhoff technique. The excitation for each dipole is delayed corresponding to transit time through the GaAs substrate and attenuated appropriately. Results are presented in Fig. 9, where comparison is made to the field found using the FDTD/Kirchhoff technique. Five dipoles are used to represent reradiation from the top and bottom edges, where advantage has been taken of the symmetry of the structure relative to the observation point. It may be seen that while the model is not exact, many of the effects of inclusion of the GaAs material may be accounted for in a very computationally efficient model. This model would be difficult to develop without comparison to a rigorous solution such as that provided by the FDTD/Kirchhoff technique.

### *B. Characterization of the Photoconducting Structure*

Building on results from the previous example, the complete photoconducting structure shown in Fig. 6 is now characterized. The dimensions of the structure are similar to those given in the last example, but with $W = 14.26$ $\mu$m and $L = 35.88$ $\mu$m. The metal strips are assumed to be perfect conductors, 1.6 $\mu$m wide, 0.23 $\mu$m thick, and separated by 10 $\mu$m. The time-varying current density in the substrate has been modeled using a combined Monte Carlo/FDTD simulation technique reported in previous work [18]. Three typical current pulses are shown in Fig. 10 to demonstrate the

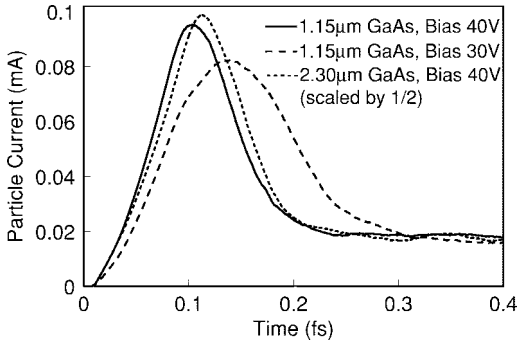


Fig. 10. Comparison of three different current pulses generated by the photoconducting experiment.

effects of varying the bias voltage and the thickness of the GaAs substrate.

These realistic current pulses contain random high-frequency content. To study effects caused by the inhomogeneous material parameters, rather than by errors in FDTD modeling, the frequency content of each pulse was limited to the degree that FDTD dispersion was not significant. This was verified by comparing the time derivative of the current pulse to the far-field radiation generated by the combined FDTD/Kirchhoff integral method for the homogeneous case.

The far-field radiation arising from two of these current pulses is presented in Figs. 11 and 12, where the fields are measured: (a) off the axis of the dipole (E-plane) and (b) transverse to the axis of the dipole (H-plane). Simulation results are

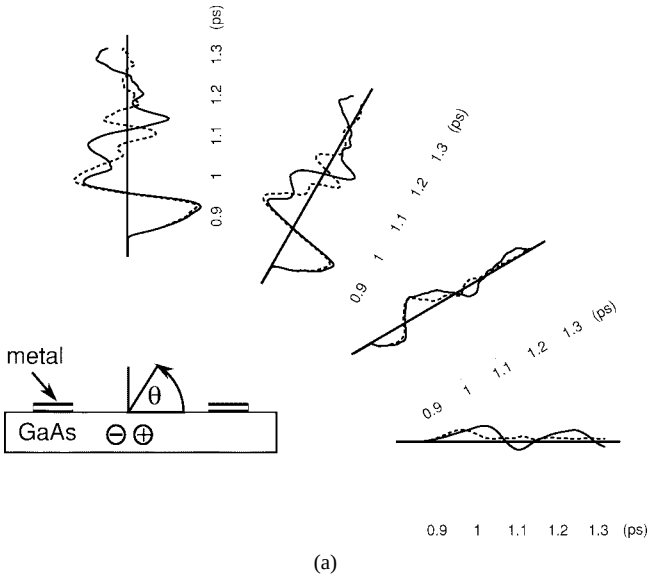


(a)

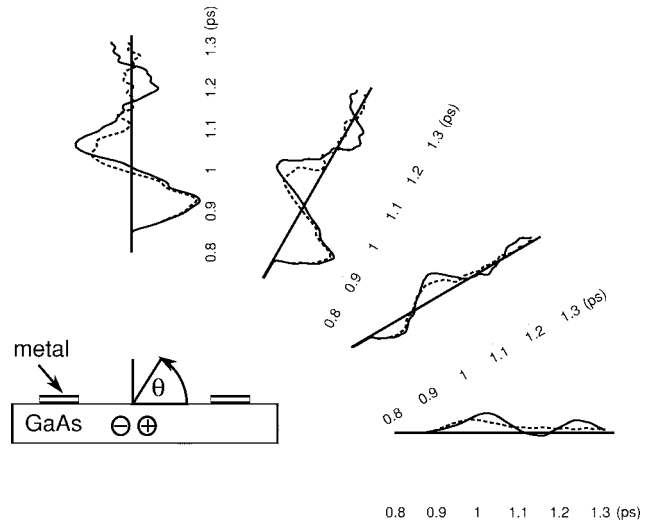


(b)

Fig. 11. E-plane comparison of the fields from (a) the narrower current pulse and (b) the wider current pulse in Fig. 10 at observation points 250 $\mu$m from the center of the structure and at angles of 0°, 30°, 60°, and 90° from the plane of the substrate and off the axis of the dipole array. The dashed lines represent the structure with the GaAs substrate only, the solid lines include the metal contacts.

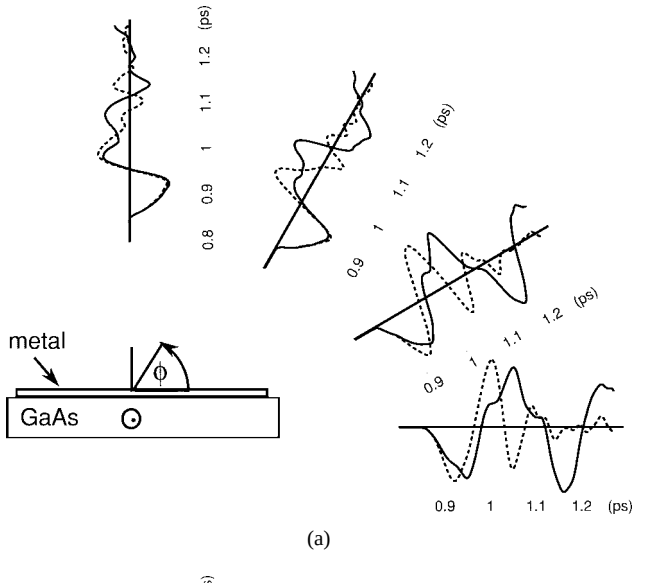


(a)

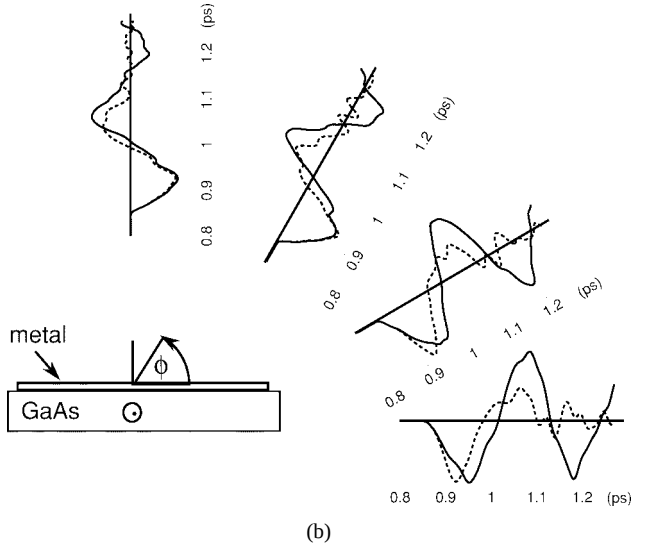


(b)

Fig. 12. H-plane comparison of the fields from (a) the narrower current pulse and (b) the wider current pulse in Fig. 10 at observation points 250 $\mu$m from the center of the structure and at angles of 0°, 30°, 60°, and 90° from the plane of the substrate and perpendicular to the axis of the dipole. The dashed lines represent the structure with the GaAs substrate only, the solid lines include the metal contacts.

presented for a narrow pulse (the solid line, 1.15 $\mu$m GaAs, Bias = 40 V, in Fig. 10) and a for wider pulse (the dashed line, 1.15 $\mu$m GaAs, Bias = 30 V, in Fig. 10). In each case the GaAs substrate is included and comparison is made with and without the metal electrodes. The narrower pulse shows more distortion due to reradiation from the edges of the GaAs substrate, particularly for the H-plane observation points.

In a homogeneous problem space, the H-plane waveforms would be identical. Effects of the metal electrodes include increased confinement of the field to the substrate region and additional distortion due to reradiation from the edges and corners of the metal. The significance of these effects is, again, pulsewidth dependent, with quite severe distortion of the field from the narrower pulse. For the wider pulsewidth, the effects of reradiation are less significant; however, the pulse is still distorted. For the narrower pulse in particular, severity of the distortion could affect timing measurements of the received signal pulse. Effects such as these due to inclusion of the material parameters would be difficult to model using other techniques, particularly for the far-field radiation.

## IV. Conclusion

A computational technique has been demonstrated which may be used to accurately and efficiently determine near- and far-field radiation from microwave and ultrafast electronic devices. The technique combines the FDTD method and the Kirchhoff surface integral in a spatial transformation. The method was validated for use in both near- and far-field calculations. Effects of the inclusion of materials in simulations of high-frequency systems was explored with an example in which a dipole source embedded in a GaAs

substrate was excited with current pulses of various durations. Pulsewidth dependent effects were shown to be significant in an application of the method to the analysis of a photoconducting structure. Additionally, the combined FDTD/Kirchhoff technique was used to develop a simple model of the radiation from an inhomogeneous structure. Further improvements to the method may include consideration of the frequency dispersive effects of the substrate material.

The combined FDTD/Kirchhoff transformation technique enables more accurate modeling and characterization of radiation from microwave and millimeter or submillimeter wave structures. The technique described here is, in many situations, more efficient than the FDTD method alone since the wave needs to propagate only to the integration surface where it is transformed in space and time to the observation point. It is expected that the technique will be of benefit in a wide range of applications.

## ACKNOWLEDGMENT

The authors would like to thank A. Wiesbauer for helpful discussions on the implementation of the Kirchhoff surface integral, and M. C. Falconer for implementation of the FDTD code.

## REFERENCES

[1] K. S. Yee, "Numerical solution of initial boundary value problems involving Maxwell's equations in isotropic media," *IEEE Trans. Antennas Propagat.*, vol. AP-14, pp. 302–307, Dec. 1966.
[2] A. Taflove, *Computational Electrodynamics: The Finite-Difference Time-Domain Method.* Boston: Artech, 1995.
[3] G. R. Kirchhoff, "Zur Theorie der Lichstrahlen," *Annalen der Physik und Chemie*, vol. 18, no. 8, pp. 663–695, 1883.
[4] B. B. Baker and E. T. Copson, *The Mathematical Theory of Huygens' Principle.* Oxford, U.K.: Oxford Univ. Press, 1939.
[5] S. A. Schelkunoff, "Some equivalence theorems of electromagnetics and their application to radiation problems," *Bell Syst. Tech. J.*, vol. 15, pp. 92–112, 1936.
[6] J. A. Stratton and L. J. Chu, "Diffraction theory of electromagnetic waves," *Phys. Rev.*, vol. 56, pp. 99–107, 1939.
[7] J. De Moerloose and D. De Zutter, "Surface integral representation radiation boundary condition for the FDTD method," *IEEE Trans. Antennas Propagat.*, vol. 41, pp. 890–896, July 1993.
[8] K. S. Kunz and R. J. Luebbers, *The Finite Difference Time Domain Method for Electromagnetics.* Boca Raton, FL: CRC Press, 1993, pp. 105–122.
[9] H. F. Harmuth, "Antennas and waveguides for nonsinusoidal waves," supp. 15 in *Advances in Electronics and Electron Physics.* New York: Academic Press, 1984, pp. 44–54.
[10] D. Buechler, D. Roper, C. Durney, and D. Christensen, "Modeling sources in the FDTD formulation and their use in quantifying source and boundary condition errors," *IEEE Trans. Microwave Theory Tech.*, vol. 43, pp. 810–814, Apr. 1995.
[11] A. Taflove, *Computational Electrodynamics: The Finite-Difference Time-Domain Method.* Norwood, MA: Artech House, 1995, pp. 40–46, 93–106.
[12] S. A. Schelkunoff, "Kirchhoff's formula, its vector analogue, and other field equivalence theorems," in *The Theory of Electromagnetic Waves: A Symposium.* New York: Interscience, 1951, pp. 43–59.
[13] C. L. Britt, "Solution of electromagnetic scattering problems using time domain techniques," *IEEE Trans. Antennas Propagat.*, vol. 37, pp. 1181–1192, Sept. 1989.
[14] K. L. Shlager and G. S. Smith, "Comparison of two FDTD near-field to near-field transformations applied to pulsed antenna problems," *Electron. Lett.*, vol. 31, pp. 936–938, Aug. 1995.
[15] J. M. Johnson and Y. Rahmat-Samii, "MR-FDTD: A multiple-region finite-difference-time domain method," *Microwave Optical Technol. Lett.*, vol. 14, pp. 101–105, Feb. 1997.
[16] O. Ramahi, "Near- and far-field calculation in FDTD simulations using Kirchhoff surface integral representation," *IEEE Trans. Antennas Propagat.*, vol. 45, pp. 753–759, May 1997.
[17] The MathWorks, *MATLAB*, vol. 5.1, Apr. 1997.
[18] S. M. Goodnick, S. Pennathur, U. Ranawake, P. M. Lenders, and V. K. Tripathi, "Parallel implementation of a Monte Carlo particle simulation coupled to Maxwell's equations," *Int. J. Num. Modeling*, vol. 8, pp. 205–219, 1995.

**Kate A. Remley** (S'92) was born in Ann Arbor, MI, in December 1959. She received the B.S.E.E. degree (*magna cum laude*) from Oregon State University, Corvallis, in 1993, and the M.S. degree in 1995. She is currently working toward the Ph.D. degree at Oregon State University.

She worked as a Broadcast Engineer in Eugene, OR, between 1983 and 1992 and was Chief Engineer of an AM/FM broadcast station from 1989–1992. Her research interests include computational modeling of radiation from microwave, millimeter-wave, and ultrafast electronic devices, modeling of wireless communication systems, and characterization of optical and quantum waveguides.

Ms. Remley was a National Science Foundation Graduate Research Fellow from 1993 to 1996.

**Andreas Weisshaar** (S'90–M'91–SM'98) received the Diplom-Ingenieur (Dipl.-Ing.) degree in electrical engineering from the University of Stuttgart, Germany, in 1987, and the M.S. and Ph.D. degrees in electrical and computer engineering from Oregon State University, Corvallis, in 1986 and 1991, respectively.

Since 1991, he has been on the faculty of the Department of Electrical and Computer Engineering at Oregon State University where he is currently an Associate Professor. His current research activities are in the areas of computer-aided design of RF/microwave circuits and components, interconnects, electronic packaging, and wireless communications.

**Stephen M. Goodnick** (M'88–SM'91) received the B.S. degree in engineering science from Trinity University in 1977 and the M.S. and Ph.D. degrees in electrical engineering from Colorado State University in 1979 and 1983, respectively.

He was an Alexander von Humboldt Fellow at the Technical University of Munich, Germany, and the University of Modena, Italy, in 1985 and 1986. He was the Melchor Visiting Chair at the University of Notre Dame in 1991. He was a faculty member from 1986 to 1997 in the Department of Electrical and Computer Engineering at Oregon State University, Corvallis, where he held the rank of Professor. He is presently Chair and Professor of Electrical Engineering at Arizona State University. He has coauthored more than 80 journal articles and book chapters related to transport in semiconductor devices and microstructures.

Dr. Goodnick is a member of the American Physical Society, Sigma Xi, and Eta Kappa Nu.

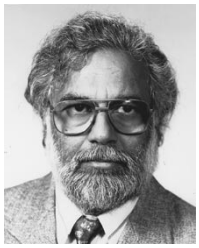

**Vijai K. Tripathi** (M'68–SM'87–F'93) received the B.Sc. degree from Agra University, India, in 1958, the M.Sc.Tech. degree in electronics and radio engineering from Allahabad University, India, in 1961, and the M.S.E.E. and Ph.D. degrees in electrical engineering from the University of Michigan at Ann Arbor in 1964 and 1968, respectively.

He is currently a Professor of Electrical and Computer Engineering at Oregon State University, Corvallis. Prior to joining Oregon State in 1974, he had been with the Indian Institute of Technology in Bombay, the University of Michigan at Ann Arbor, and the University of Oklahoma, Norman. His visiting and sabbatical appointments include the Division of Network Theory, Chalmers University of Technology, Gothenburg, Sweden (1981–1982), Duisburg University, Duisburg, Germany (1982), the Naval Research Laboratory, Washington, DC (1984), and the University of Central Florida, Orlando, (Fall 1990). Over the years, he has been a consultant to many industrial organizations, including AVANTEK, EEsof, Inc., Teledyne MMIC, and Tektronix. His research activities are in the general areas of RF and microwave circuits, computational electromagnetics, electronic packaging, and interconnects.